

Indoor Localization Method of Mobile Educational Robot Based on Visual Sensor

Wei ping Zhu¹, Xiaoling Cheng^{2*}

¹ School of Humanities and Education, Nanchang Institute of Technology, China

² School of Electronics and Information, Nanchang Institute of Technology, China
zhuweiping1991410@163.com, cxl@nut.edu.cn

Abstract

This article aims to study the mobile positioning method of mobile educational robots indoors. In order for robots to be able to unblocked indoors, they can avoid obstacles well. Vision sensors are the direct source of information for the entire machine vision system, and are mainly composed of one or two graphics sensors, sometimes accompanied by light projectors and other auxiliary equipment. This paper presents an indoor positioning method for mobile educational robots based on visual sensors. Build some models to compare which algorithm is more in line with the positioning of indoor mobile educational robots. The experimental results in this paper show that the positioning accuracy of the optical flow meter and the odometer on the short-haired carpet is equivalent (both are less than the index 4.52%); the positioning error of the optical flowmeter on the long-haired carpet is the largest 7%, and the positioning error of the odometer is the largest it reached 83%. The error of the algorithm positioning method after the visual odometer fusion is obviously smaller than that of the optical flow method. This shows that the algorithm after visual process fusion is more suitable for indoor mobile educational robot positioning than this optical flow method.

Keywords: Visual sensor, Mobile educational robot, Indoor positioning, Visual odometer

1 Introduction

1.1 Background

Position and attitude estimation is a very important basic problem in the fields of mobile educational robots, unmanned driving, aerospace, navigation and other fields. Foreign research on robot positioning involves the application of robot positioning in online maps and map construction. The most common absolute positioning is the global positioning system. This positioning method is mature and can provide absolute positioning without cumulative errors. However, weather conditions, obstacles, indoor environment and other factors will affect the GPS signal reception. In indoor scenarios, GPS-based absolute positioning methods are not applicable and have low accuracy; methods based on wireless signals or scene tags need to arrange scenes in advance, which is not

highly scalable and difficult to promote. The relative positioning method is based on the initial position of the robot, and calculates the change of its position and posture according to the movement of the robot at each moment. In order to better allow the mobile educational robot to move smoothly in indoor scenes, he can avoid obstacles according to his own judgment, so as to really help us.

1.2 Significance

The vision of a mobile robot is an important part of the robot system. When the robot has the function of visual perception, the robot can obtain the image of the environment through the optical sensor in the vision system, and after a series of processing and analysis, it is converted into symbols that the robot can recognize, so that the robot can recognize objects based on this information. In many applications, such as deep-water exploration, space exploration, space operations, etc., there is no external sensor to provide the robot's global information. Based on the robot's own configuration of visual sensors, the robot's position and posture can be evaluated online and the environment in which the robot is encountered is affected. It is of great significance to improve the operational capabilities of mobile robots these more dangerous scientific research work can be done slowly instead of us, so that they will not bring life danger to the researchers, and they can also be used in our lives to help us answer children's questions and act as tutors Responsibilities and so on. It will become more intelligent in the future.

1.3 Related Work

Now more and more robots have entered our lives. In Karaahmetolu K's research, their team proposed applying arduino educational robots to students' computational thinking skills and their perception of Basic Stem skill levels. Although their experiments are very forward-looking, there are still some technical problems [1]. In X. Wang's research, their team developed an improved RBPF algorithm based on a distributed sphere algorithm proposed by the fusion calculation of observation data (optical information or radar information) and odometer information to speed up optical image processing speed. In the experiment, their team's consideration was not comprehensive enough, which led to the controversy of the experimental results [2]. In L. Yao's research, their team proposed a method based on tight coupling and nonlinear optimization, combined with the measured val-

*Corresponding Author: Xiaoling Cheng; E-mail: cxl@nut.edu.cn

ues of the pre-integrated inertial measurement unit, to obtain a high-precision vision positioning solution. Although their research is very forward-looking, there are still some flaws in the research. For example, the experimental process is more complex and not easy to operate [3]. In M. J. Lim's research, they proposed to design a location information service system based on the Internet of Things for a new generation of enjoying cultural life. However, in the process of experimental research, there are still some influencing factors that affect the results that have not been resolved, so the results obtained still have certain imperfections [4]. In Y. Song's research, they proposed a wireless sensor network (WSN)-based system scheme, using Atmega128L chip and TI's low-power RF chip CC2530, to design the sink node and sensor node. Their research has great practical value, but their technology is not very mature yet and needs to be further strengthened [5]. In A. Bautista's research, he pointed out that there are still some differences between mobile educational robots and offline educational robots, but they are still very helpful in helping children learn [6]. In Xiaobo Wu's research, he proposed a thesis on a mobile robot composed of omnidirectional wheels, and analyzed the material structure and dynamics of the four-wheel omnidirectional robot. This experiment is very helpful to our current study and life, but it is obvious that there are still insufficient comprehensive problems, which need to be further strengthened and supplemented [7].

1.4 Innovation

According to the technical requirements of this project, this article is dedicated to improving the accuracy, reliability and real-time estimation of the robot's posture, focusing on the rapid extraction of features, camera mapping and parameter calibration. The research results can be widely used in various mobile [https://translate.google.cn/autonomous robots](https://translate.google.cn/autonomous%20robots) to improve the working ability of autonomous mobile training robots. When mobile educational robots combine the application of visual sensors, they can help students solve more problems. However, Mobile education robots also have some shortcomings, such as in human intelligence is not good enough.

2 Various Technical Theories and Methods

2.1 Application of Vision Sensor

In the research of sensor technology, the development of vision technology is relatively mature compared to other functions, and the application on robots is relatively complete [8-9]. Poor performance or failure to meet the requirements will affect the robot [10]. The optical sensor is equivalent to the human eye. The structure diagram of the optical sensor in the mobile training robot is shown in Figure 1 [11].

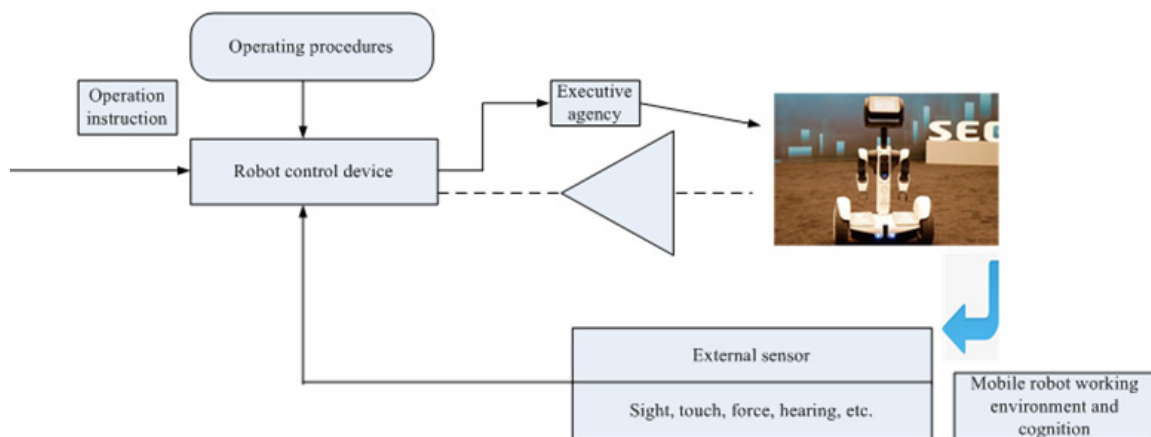


Figure 1. The role of vision sensors in mobile educational robots

As shown in Figure 1, the mobile training robot is the most critical part of the entire SLAM system.

2.2 Various Key Theories

The apparent motion of this image brightness state is the luminous flux, and the luminous flux represents the change of the image [12]. The two-dimensional velocity vector is the projection of the three-dimensional velocity vector of the viewpoint on the scene of the imaging surface. Optical flow research has very important applications in robot fragmentation, recognition, tracking, navigation, and extraction of 3D structure and motion from visual flow [13]. The traditional optical flow meter is shown in Figure 2, and the frame rate of the image is the image taken per second by the camera of the

optical flow meter. The higher the frame rate of the image, the lower the detectable low motion and the faster the recognition speed [14]. Autonomous positioning is the core part of the mobile robot positioning and navigation system. Whether indoor or outdoor, mobile robots can complete upper-level tasks such as navigation, autonomous obstacle avoidance, path planning, image recognition, and autonomous driving through precise positioning. When the body is in a static state, it will also be interfered by factors such as zero drift, and when the mobile robot is in an indoor environment, satellite GPS cannot be used. At this time, the importance of the odometer based on the vision sensor is even more prominent.

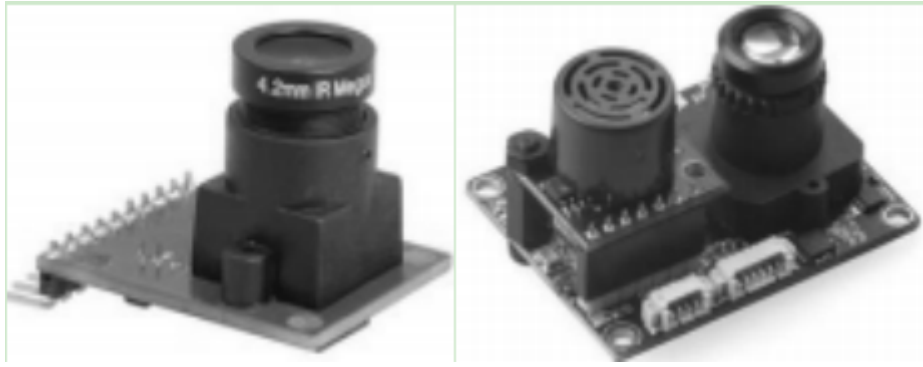


Figure 2. Traditional optical flow meter

When navigating, the odometer uses actuator data to estimate changes in position over time. Although traditional odometer technology is useful for wheeled or tracked vehicles, it is not suitable for non-standard robots. Optical odometry uses continuous camera images to estimate the distance traveled to determine equivalent information [15]. Optical odometers allow robots or vehicles to use any type of motion on any surface to improve navigation accuracy. Optical odometer is an important part of SLAM optical system. The main difference between VO and v-slam is that VO only focuses on the positioning function, while the integrated closed system not only uses the VO position, but also uses post-optimization, mapping and loop detection functions [16]. The movement process of the carrier can be estimated by continuously accumulating movement changes. Accompanying this process is the accumulation of errors caused by each estimation, so the accuracy of the visual odometer will continue to decrease over time [17]. In a complete SLAM system, the main task of the loopback detection part is to reduce the error accumulation of the front-end visual odometer. The complete SLAM system block diagram is shown as in Figure 3.

The R200 is an optical stereo vision system that uses an active structure to calculate the depth. The stereo vision system consists of a left infrared camera, a right infrared camera and an infrared laser transmitter. The laser transmitter projects fringes into the environment to increase the texture complexity of the scene, and then the left and right infrared cameras collect binocular stereo images. Finally, the Specific Integrated module mounted on the R200 module calculates the parallax and outputs the depth map. The infrared laser transmitter greatly improves the R200's ability to measure the depth of low-texture scenes. The working process of R200 is shown in Figure 4 [18]. When the characteristics of the projection light source are fixed, the size of the spot is proportional to the distance between the object and the camera, and the accuracy of the measurement is inversely proportional to the distance. Therefore, depth cameras based on active projection are generally used for close range measurement. Moreover, it is only suitable for corresponding positioning indoors. Outdoors, because outdoor light will affect its judgment and cause relatively large errors, this camera is only suitable for indoor scenes [19-20].

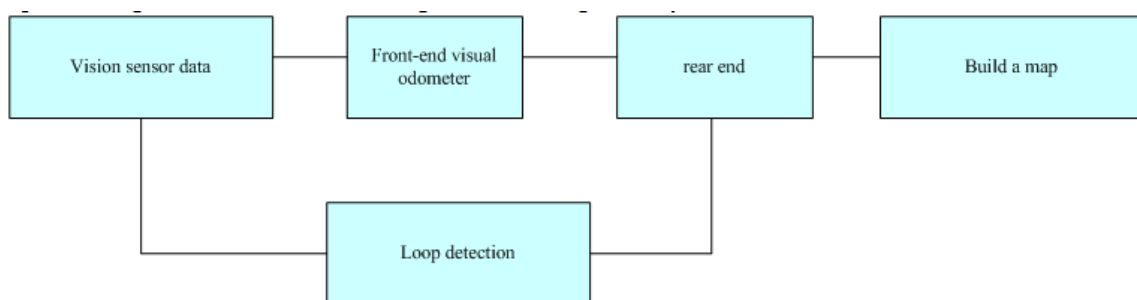


Figure 3. SLAM system block diagram

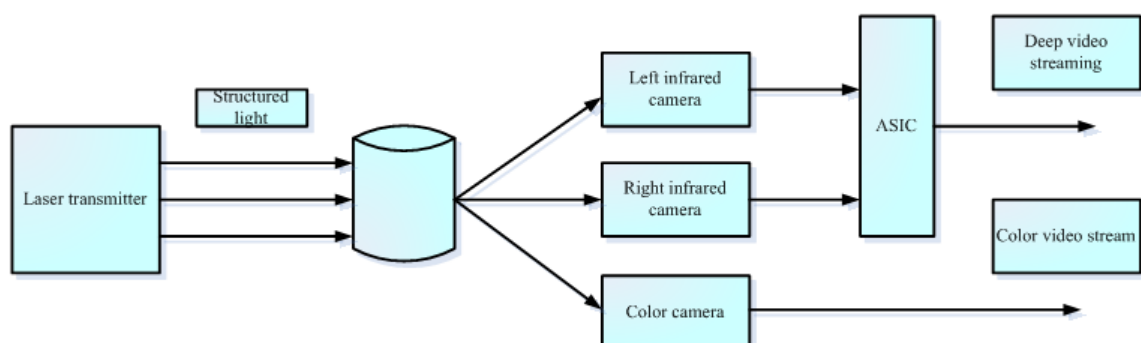


Figure 4. Working process of R200

2.3 Establishment of Mobile Educational Robot System Model

In order to create a more systematic mobile training robot system and ensure the reliability and real-time performance of the system, this article uses rapid image optimization technology to process the collected images [21]. The divided image will have noise. This paper uses the method of removing image interference and defines the mathematical model of morphology. The Harris angle detection method based on the scale space theory is used in the construction process,

which can ensure that the angle is not affected by the light conditions and the change of the camera position [22]. After the robot enters the area, it will match the positioning map, update the map according to the changes in the environment, and realize navigation. Electronic products, pre-school media, and educational robots are highly interactive, and can be used as children's companions to relieve the loneliness of the only child to a certain extent, cultivate children's innovative thinking, and contribute to the teaching of mathematics, engineering and other subjects.

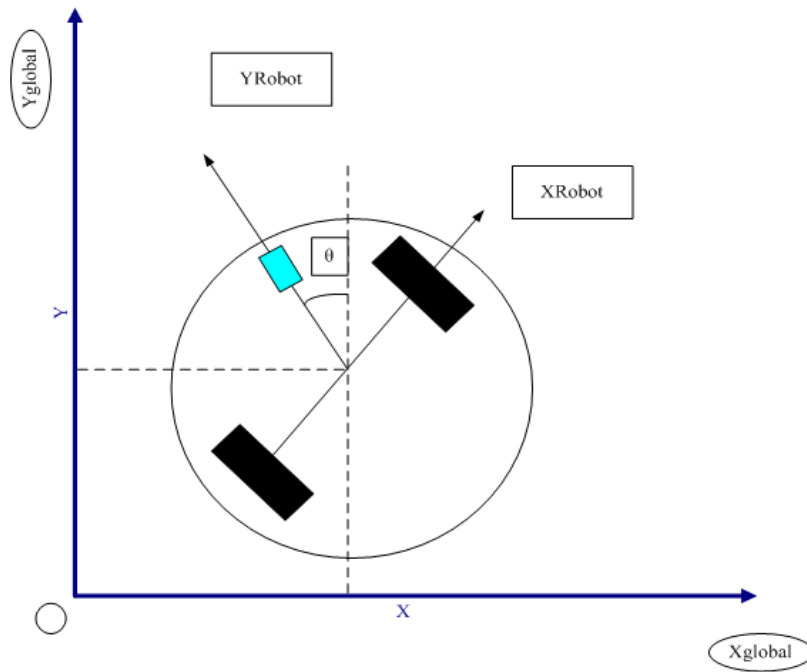


Figure 5. Mobile educational robot coordinate system

For the schematic information of the robot in the overall reference coordinate system, the relationship between the robot coordinate system and the global reference coordinate system needs to be determined, as shown in Figure 5. XGlobal, yglobal, xrobot, and yrobot are the axes of the coordinate system. The position of the robot in the reference coordinate system can be determined by the point P (x, y) and the angle. Therefore, their position can be represented by three variables X, y, θ .

$$\sigma_{global} = \begin{bmatrix} x \\ y \\ \theta \end{bmatrix}. \quad (1)$$

$$R(\theta) = \begin{bmatrix} \cos \theta & \sin \theta & 0 \\ -\sin \theta & \cos \theta & 0 \\ 0 & 0 & 1 \end{bmatrix}. \quad (2)$$

$$\dot{\sigma}_{robot} = R(\theta) \dot{\sigma}_{Global}. \quad (3)$$

The mobile robot is driven by a two-wheel differential. The distance between the two wheels is L. The robot's movement is determined according to its speed (v) and angular speed (ω).

$$\dot{\sigma}_{global} = \begin{bmatrix} \dot{x} \\ \dot{y} \\ \dot{\theta} \end{bmatrix} = f(v, \omega). \quad (4)$$

$$\dot{\sigma}_{global} = R(\theta)^{-1} \begin{bmatrix} V \\ 0 \\ \omega \end{bmatrix}. \quad (5)$$

So we can express the movement of the mobile educational robot by the following kinematic model as

$$\dot{\sigma}_{\text{global}} = \begin{bmatrix} \dot{x} \\ \dot{y} \\ \dot{\theta} \end{bmatrix} = \begin{bmatrix} v \sin \theta \\ v \cos \theta \\ \omega \end{bmatrix}. \quad (6)$$

The kinematics model of the mobile robot can be expressed as follows:

$$\dot{x} = \begin{bmatrix} \dot{x} \\ \dot{y} \\ \dot{\theta} \\ \dot{v} \\ \dot{\omega} \end{bmatrix} = \begin{bmatrix} v \sin \theta \\ v \cos \theta \\ \omega \\ 0 \\ 0 \end{bmatrix}. \quad (7)$$

The model of the discretization post-processing system is as follows:

$$x_k = \begin{bmatrix} x_k \\ y_k \\ \theta_k \\ v_k \\ \omega_k \end{bmatrix} = \begin{bmatrix} x_{k-1} - v_{k-1} \Delta t \sin \theta_{k-1} \\ y_{k-1} - v_{k-1} \Delta t \cos \theta_{k-1} \\ \theta_{k-1} + \omega_{k-1} \Delta t \\ v_{k-1} \\ \omega_{k-1} \end{bmatrix}. \quad (8)$$

2.4 The Establishment of the Visual Sensor Observation Model

$$v_r = \Delta c_r / \Delta t = \frac{2v + \omega l}{2}. \quad (9)$$

$$v_l = \Delta c_l / \Delta t = \frac{2v - \omega l}{2}. \quad (10)$$

In the above formula, v_r and v_l are the translational speeds of the left and right wheels, v and ω are the linear velocity and angular velocity of the robot center, respectively. Therefore, the observation model of the odometer is:

$$h_{\text{encoder}} = \begin{bmatrix} v_r \\ v_l \end{bmatrix} = \begin{bmatrix} v + \omega l / 2 \\ v - \omega l / 2 \end{bmatrix}. \quad (11)$$

$$h_{\text{encoder}} = \begin{bmatrix} 0 & 0 & 0 & 1 & l/2 \\ 0 & 0 & 0 & 1 & -l/2 \end{bmatrix}. \quad (12)$$

After being transformed into:

$$g_k = h_{\text{encoder}} x_k + u_k. \quad (13)$$

2.5 Optical Flow Meter Measurement Model

Installing a sensor on the mobile robot to sense its position changes can also help it to make more scientific and effective judgments.

$$v_x = \Delta x / \Delta t = \omega d. \quad (14)$$

$$v_y = \Delta y / \Delta t = v. \quad (15)$$

The installation position on the experimental platform is shown in Figure 6.

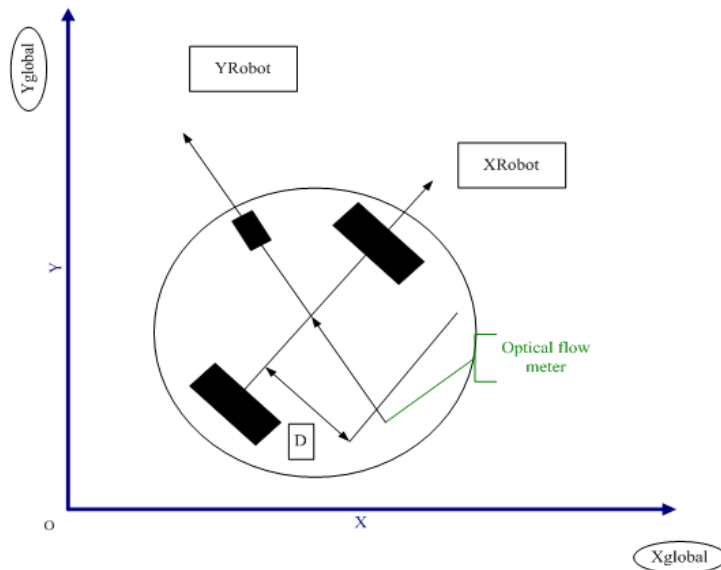


Figure 6. The installation position of the optical flow meter on the robot experimental platform

So we can get that the observation model of the optical flow meter is:

$$\mathbf{h}_{\text{optical_flow}} = \begin{bmatrix} v_x \\ v_y \end{bmatrix} = \begin{bmatrix} \omega d \\ v \end{bmatrix}. \quad (16)$$

The corresponding observation model Jacobian matrix is:

$$\mathbf{h}_{\text{optical_flow}} = \begin{bmatrix} 0 & 0 & 0 & 0 & d \\ 0 & 0 & 0 & 1 & 0 \end{bmatrix}. \quad (17)$$

After a certain transformation, you can get:

$$\mathbf{g}_k = \mathbf{h}_{\text{optical_flow}} \mathbf{x}_k + \mathbf{v}_k. \quad (18)$$

2.6 IMU Measurement Model

For indoor mobile educational robots, the gyroscope only needs to measure the angular velocity of the mobile robot's Z axis. So we can get the corresponding IMU angular velocity observation model as:

$$\mathbf{h}_{\text{IMU}} = [\omega_{\text{IMU}}] = \omega. \quad (19)$$

The corresponding observation model Jacobian matrix is:

$$\mathbf{h}_{\text{IMU}} = [\omega_{\text{IMU}}] = \omega. \quad (20)$$

After a certain transformation, we get:

$$\mathbf{g}_k = \mathbf{h}_{\text{imu}} \mathbf{x}_k + \mathbf{v}_k. \quad (21)$$

By integrating the angular velocity, we can get the azimuth angle θ of the robot, and then we can get the angle observation model of imu as:

$$\mathbf{h}_{\text{heading}} = \int \omega_{\text{imu}} dt = \theta. \quad (22)$$

$$\mathbf{h}_{\text{heading}} = [0 \ 0 \ 1 \ 0 \ 0]. \quad (23)$$

After simplification, we can get:

$$\mathbf{g}_k = \mathbf{h}_{\text{heading}} \mathbf{x}_k + \mathbf{v}_k. \quad (24)$$

3 Error Analysis of Mobile Comparison Experiment

3.1 Experimental Equipment

Now more and more intelligent robots have entered our more and more homes. An ordinary intelligent robot was randomly selected for this experiment. On the robot platform, we open programming interfaces to users for experimental mobile the main performance of educational robots is shown in Table 1.

Table 1. Various performance introduction

Parameter	Numerical value
Overall size	Diameter 645.32mm, height 300mm
Axle length	345mm
Wheel diameter	99mm
Encoder pulse number	708.2/rev
Serial port baud rate	115200Bd/s
Wheel speed range	-500 ~ 500mm/s

We build the same physical map environment as the simulation map. We use the existing robot platform and two-dimensional laser technology to build the environment map by installing IMU modules, optical flow sensors, Bluetooth modules, controllers, and camera modules on the experimental robot platform. And embedded R16 platform to meet the positioning requirements of indoor mobile educational robots. The odometer information is obtained by directly reading the left and right encoder pulses. The hardware platform structure diagram of the mobile educational robot is shown in Figure 7.

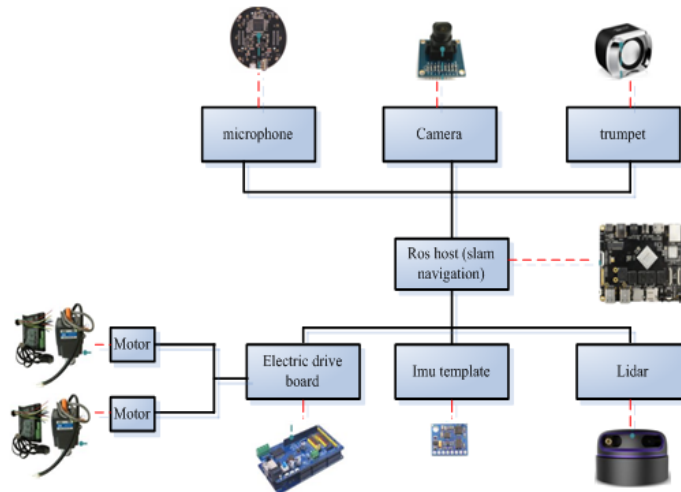


Figure 7. Hardware platform structure diagram of mobile educational robot

3.2 Move Experiment on Different Materials

In order to compare the actual performance of the optical flow meter and the odometer on the surface of different materials, this experiment will be carried out on the short-haired carpet and the long-haired carpet on the surface of two different materials, and the actual displacement of the robot and the fusion of the optical flow meter will be recorded respectively. The trajectory displacement fused with the odometer (this experiment uses the distance of the robot's forward direction

as the recorded value). The experimental requirements are for manually controlling the robot to advance a specified distance. When moving on the short-haired carpet, his trajectory diagram is shown in Figure 8, and the coordinate points and error analysis are shown in Table 2.

The fusion trajectory of the robot on the long-haired carpet is shown in Figure 9, and the coordinate point recording and error analysis are shown in Table 3.

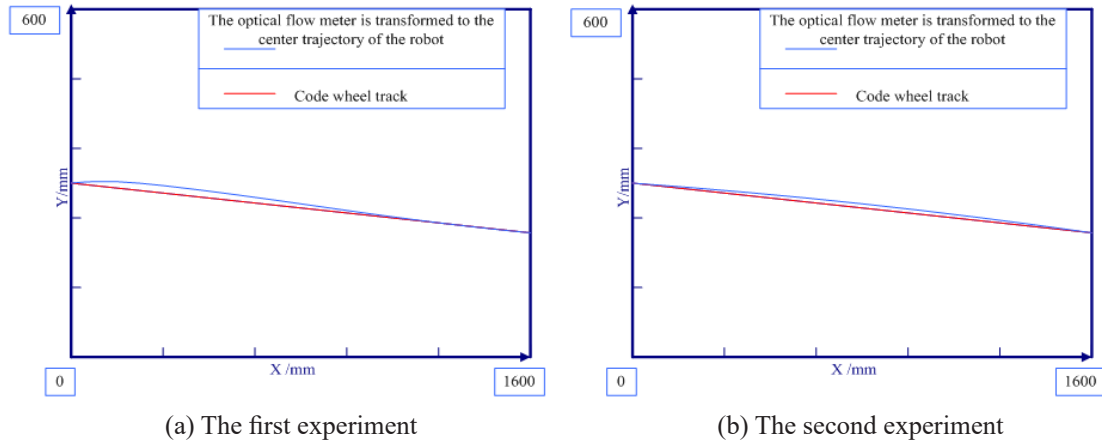


Figure 8. Comparison experiment of fusion trajectory of short wool blanket

Table 2. Short-haired carpet fusion coordinates and errors

Number of experiments	Actual displacement	Optical flow meter fusion	Error	Odometer fusion	Error
The first time	1720	1779	59 (3.4%)	1788	68 (4.0%)
The second time	1750	1764	14 (0.8%)	1786	36 (2.1%)
The third time	1780	1820	40 (4%)	1799	21 (1.6%)

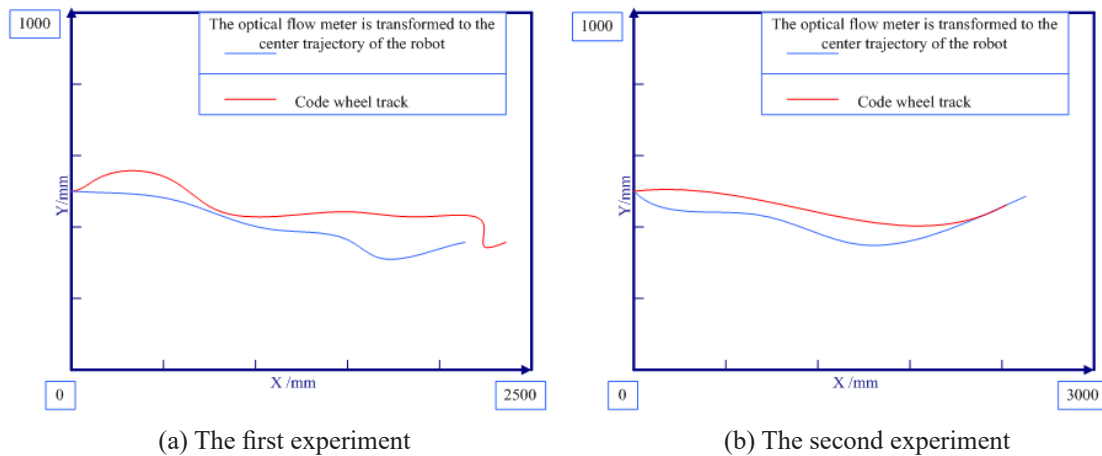


Figure 9. Comparative experiment of long-haired carpet fusion trajectory

Table 3. Long-haired carpet fusion coordinates and errors

Number of experiments	Actual displacement	Optical flow meter fusion	Error	Odometer fusion	Error
The first time	1800	1946	146 (7%)	2999	1199 (68%)
The second time	1800	1870	66 (4%)	3310	1510 (83%)
The third time	1800	1899	99 (5%)	3210	1410 (82.6%)

3.3 Analysis of Experimental Results

Using the motion estimation method, the position and direction of the camera with better robustness can be finally obtained, and the camera is the vision camera of the robot, so the result obtained is the pose information of the robot. In order to make the final positioning result have high accuracy and good real-time performance, high-precision point extraction, more accurate feature combinations, more accurate and smaller feature point pairs, and better motion estimation methods are required. These papers carried out research and simulation experiments on the last point, and compared the research results with the simulation experiments and verified them. The system has high positioning efficiency, good real-time performance and good stability.

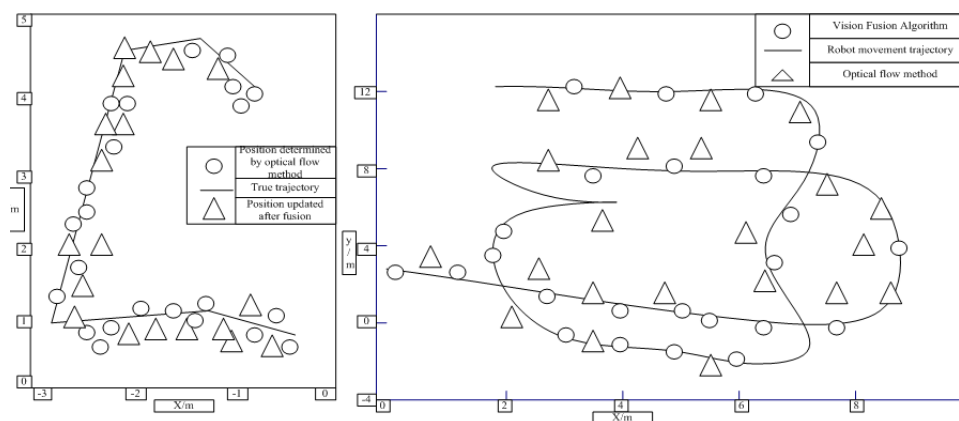
From the comparison results of Table 2 and Table 3, it can be seen that the positioning accuracy of the optical flow meter and the odometer on the short-haired carpet are equivalent (both are less than the index 4.52%); the positioning error of the optical flow meter on the long-haired carpet is the largest 7%, and the maximum positioning error of the odometer reaches 83%. On the other hand, the trajectories in Figure 8 and Figure 9 also conform to the actual trajectory shape. Therefore, the experimental results confirm that the optical flow meter can provide more accurate positioning information on different material surfaces, while the odometer is almost in a state of failure on the long-haired carpet (in the case of slipping) and cannot provide positioning information. On the other hand, it shows that the scale information of the relative position sensor on the surface of different materials is different, but the scale information of the optical flow meter is more stable. So far, the positioning problem of indoor robots is still one of the core problems in the current robotics research field, and the focus of future work is to improve the positioning accuracy of the robot and fully realize the autonomous positioning of the robot, and improve the application of the positioning algorithm stability, rapidity and effectiveness. Robot positioning adopts the SLAM method to implement real-time construction of unknown environment maps, which are applied to map matching positioning, and the study

of more efficient resampling and adaptive sampling particle filter positioning algorithms has a good application prospect. On the whole, the whole process is relatively smooth, but the efficiency of the experiment is not high enough, hope the experimental efficiency can be improved in the future.

4 Results Discussion

4.1 Visual Odometer Positioning Estimation Trajectory

It can be seen from Figure 10 that it can be intuitively seen from the figure that when the movement is just started, the local map is initialized, and the time flow method and the real trajectory are not large when walking in a straight line. The visual fusion with the feature point matching algorithm makes the position estimation more effective. However, when the robot turns, the pose information estimated by the optical flow method is quite different from the real situation at this time, and the advantages of algorithm fusion are reflected. As shown in the two more obvious inflection points in the above figure, the position estimated by the optical flow method is farthest away from the true position by 0.15m, and the error accumulation tends to become larger as time goes by. However, due to the existence of a local map, the feature point matching between the frame and the key frame can be regarded as a strong motion estimation constraint, eliminating errors as much as possible, bringing the estimated position close to the real trajectory again, and passing it as the initial value to the algorithm fusion at the next moment Stage to avoid accumulation of errors. The result of the fusion is more detailed than the simple feature point matching and positioning algorithm, and can provide more information, especially when the texture is not obvious, the optical flow tracking method can be used to realize the positioning. Correspondingly, compared with the pure optical flow method, because the feature point matching algorithm is introduced as a correction, the robot turning out angle estimation is more accurate, and the feature point matching can be used to assist positioning when the light intensity changes greatly.



(a) Visual odometer fusion algorithm positioning result (b) Visual odometer position estimation in indoor scene

Figure 10. Visual odometer positioning estimated trajectory

4.2 Errors of Different Visual History Algorithms

As shown in Figure 11, when we have a time guarantee, in order to further analyze the accuracy and reliability of the visual fusion algorithm, we will now analyze the error curve of the algorithm. The error curve is the Euclidean distance between the position of the mobile robot obtained by the visual mileage calculation method and the motion capture system (true value). It can be seen that the linear walking time flow method provides a fast positioning method under the condition of ensuring accuracy. When a turn occurs, the positioning accuracy error after the correction of the visual odometer fusion algorithm is significantly smaller than the error caused by the optical flow method. This shows that the visual odometer fusion algorithm has a more accurate application effect than the optical flow method.

4.3 Visual Inertial Fusion Framework

As shown in Figure 12, using the characteristics of ROS, the program functions are decoupled, and the image data

is processed in a separate node `feature_tracker`. The node completes the feature point extraction of the visual part and restores the camera movement, and then sends the paired feature point information to another node `vins_estimator` in the form of a ROS message. Another node `vins_estimator` subscribes to the IMU data from the sensor, and then pre-integrates the data to construct the residual error of the IMU item; at the same time subscribes to the message sent by the `feature_tracker` to construct the reprojection error item of the feature point. Then, use Google ceres-solver to solve the objective function, iterative optimization is the smallest objective function, and the output result is the carrier pose. Since the visual and inertial fusion has more system states, in order to limit the scale of the optimization problem, the optimization of the system adopts an optimization strategy based on a sliding window. The key to the visual fusion algorithm is in fusion, that is, the fusion use of various visual optimization methods and strategies.

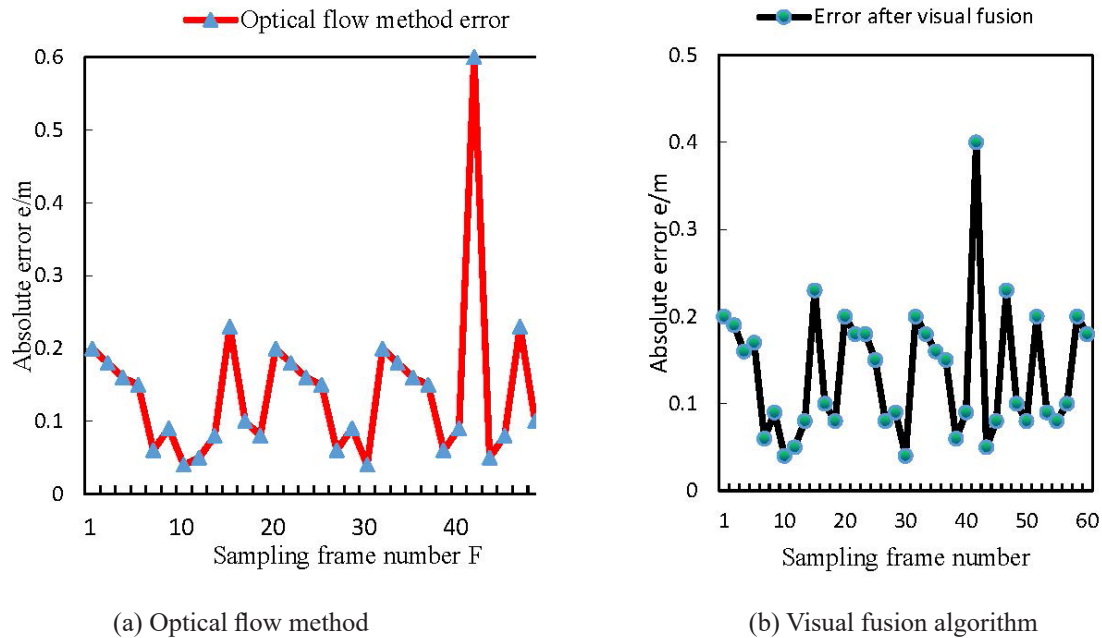


Figure 11. Errors of different visual history algorithms

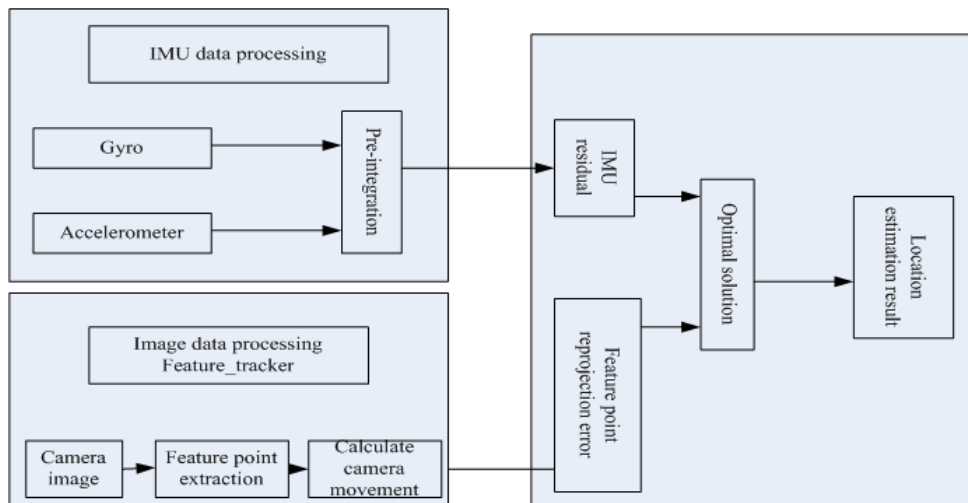


Figure 12. Visual-inertial fusion framework

5 Conclusions

With the development of the times, the era of highly intelligent mobile robots has arrived. This paper studies the positioning of mobile educational robots based on vision sensors. The positioning method based on the fusion of vision and inertia can be adapted to a wider range of sensor types. The experimental results verify the performance and effectiveness of the visual inertial odometer, indicating that it is a practical indoor positioning method. Multiple sensor information sources make the system more accurate. The performance of the hardware restricts the overall performance of the system more severely. Especially the performance of the gyroscope will affect the performance of the system during rotation. The limitations of the positioning environment, positioning accuracy, and real-time performance still need to be improved. The research results prove that in the future, the application of visual sensors in the field of more and more widely in mobile educational robots.

Acknowledgements

This work was supported by Jiangxi Provincial Department of Education Science and Technology Research Project-Indoor Positioning Research for Educational Robots (GJJ202119).

References

- [1] K. Karaahmetoglu, Ö. Korkmaz, The Effect of Project-Based Arduino Educational Robot Applications on Students' Computational Thinking Skills and Their Perception of Basic Stem Skill Levels, *Participatory Educational Research*, Vol. 6, No. 2, pp. 1-14, December, 2019.
- [2] X. Wang, L. He, T. Zhao, Mobile Robot for SLAM Research Based on Lidar and Binocular Vision Fusion, *Chinese Journal of Sensors and Actuators*, Vol. 31, No. 3, pp. 394-399, March, 2018.
- [3] L. Yao, F. Li, Mobile Robot Localization Based on Vision and Multisensor, *Journal of Robotics*, Vol. 2020, No.5, pp. 1-11, June, 2020.
- [4] J. M. Lim, J. Y. Nam, M. Y. Kwon, Design of Location Information System Using a IoT-based on Sensor, *Journal of Engineering and Applied Sciences*, Vol. 13, No. 3, pp. 639-642, 2018.
- [5] Y. Song, X. Zhang, M. Zhang, J. Wang, Research of Node Localization Algorithm Based on Wireless Sensor Networks in Marine Environment Monitoring, *Journal of Computational Methods in Sciences & Engineering*, Vol. 18, No. 1, pp. 69-83, February, 2018.
- [6] A. Bautista, Blended Online and Offline Robotics Learning Program Using Low-Cost Mobile Educational Robot, *International Journal of Advanced Trends in Computer Science and Engineering*, Vol. 9, No. 1.1 SI, pp. 278-282, February, 2020.
- [7] X. B. Wu, Z. Chen, W. B. Chen, W. K. Wang, Research on the Design of Educational Robot with Four-Wheel Omni-Direction Chassis, *Journal of Computers (Taiwan)*, Vol. 29, No. 4, pp. 284-294, August, 2018.
- [8] M. Pan, Y. Liu, J. Cao, Y. Li, C. Li, C.-H. Chen, Visual Recognition Based on Deep Learning for Navigation Mark Classification, *IEEE Access*, Vol. 8, pp. 32767-32775, February, 2020.
- [9] S. Zhou, M. Ke, P. Luo, Multi-camera transfer GAN for person re-identification, *Journal of Visual Communication and Image Representation*, Vol. 59, pp. 393-400, February, 2019.
- [10] F. Lopez-Rodrigues, F. Cuesta, Andruino-A1: Low-Cost Educational Mobile Robot Based on Android and Arduino, *Journal of Intelligent & Robotic Systems: Theory & Application*, Vol. 81, No. 1, pp. 63-76, January, 2016.
- [11] M. Z. Zhang, L. M. Wang, S. M. Xiong, Using Machine Learning Methods to Provision Virtual Sensors in Sensor-Cloud, *Sensors*, Vol. 20, No. 7, Article No. 1836, April, 2020.
- [12] H. Song, M. Brandt-Pearce, A 2-D Discrete-Time Model of Physical Impairments in Wavelength-Division Multiplexing Systems, *Journal of Lightwave Technology*, Vol. 30, No. 5, pp. 713-726, March, 2012.
- [13] A Shariati, A. H. Shamekhi, A. Ghaffari, S. Gholampour, A. Motaghd, Conceptual Design Algorithm of a. Two-Wheeled Inverted Pendulum Mobile Robot for Educational Purposes, *Mechanics of Solids*, Vol. 54, No. 4, pp. 614-621, July, 2019.
- [14] I. Bula, E. Hajrizi, Cost Oriented Autonomous Mobile Service Robot, *IFAC-PapersOnLine*, Vol. 52, No. 25, pp. 91-94, 2019.
- [15] T. Phetsrikrarn, W. Massagram, A. Harfield, First Steps in Teaching Computational Thinking through Mobile Technology and Robotics, *Asian International Journal of Social Sciences*, Vol. 17, No. 3, pp. 37-52, July, 2017.
- [16] M. Elhoseny, Multi-object Detection and Tracking (MODT) Machine Learning Model for Real-Time Video Surveillance Systems, *Circuits, Systems, and Signal Processing*, Vol. 39, No. 2, pp. 611-630, February, 2020.
- [17] Y. Tang, G. Han, K. Hu, S. Lu, T. Wu, Design of a New Type of Small Wireless Active Omni-Directional Vision Sensor, *Yi Qi Yi Biao Xue Bao/Chinese Journal of Scientific Instrument*, Vol. 37, No. 3, pp. 553-560, March, 2016.
- [18] G. Chen, F. Wang, X. Yuan, Z. Li, Z. Liang, A. Knoll, NeuroBiometric: An Eye Blink Based Biometric Authentication System Using an Event-Based Neuromorphic Vision Sensor, *IEEE/CAA Journal of Automatica Sinica*, Vol. 8, No. 1, pp. 206-218, January, 2021.
- [19] E. Mohamed, The Relation of Artificial Intelligence with Internet of Things: A survey, *Journal of Cybersecurity and Information Management*, Vol. 1, No. 1, pp. 30-34, January, 2020.
- [20] M. Suárez, V. M. Brea, J. Fernández-Berni, R. Carmona-Galan, D. Cabello, A. Rodríguez-Vázquez, Low-Power CMOS Vision Sensor for Gaussian Pyramid Extraction, *IEEE Journal of Solid-State Circuits*, Vol. 52, No. 2, pp. 483-495, February, 2017.
- [21] J. A. Lenero-Bardallo, P. Hafliger, R. Carmona-Galan,

- A. Rodriguez-Vazquez, A Bio-Inspired Vision Sensor with Dual Operation and Readout Modes, *IEEE Sensors Journal*, Vol. 16, No. 2, pp. 317-330, January, 2016.
- [22] S. Lee, G. Tewolde, J. Lim, J. Kwon, Vision Based Localization for Multiple Mobile Robots Using Low-cost Vision Sensor, *International Journal of Handheld Computing Research*, Vol. 7, No. 1, pp. 12-25, January, 2016.

Biographies



Weiping Zhu was born in Anqing, Anhui, China, and received a master's degree in education from Dhurakij Pundit University in Thailand. She is currently an assistant professor at Nanchang Institute of Technology, and her research work focuses on education technology and education management.



Xiaoling Cheng was born in Tongling, Anhui, China. She received her bachelor's degree from Nanchang Institute of Technology and her master's degree from Ban-somdejchaopraya Rajabhat University in Thailand. She is now an assistant researcher at Nanchang Institute of Technology. Her research focuses on the application of robotics in education.